The Journal of Experimental Biology 208, 3065-3073
Published by The Company of Biologists 2005
doi:10.1242/jeb.01752

Spike firing allometry in avian intrapulmonary chemoreceptors: matching neural code to body size

S. C. Hempleman[1,*], D. L. Kilgore, Jr[2], C. Colby[3], R. W. Bavis[4] and F. L. Powell[5]

[1]*Department of Biological Sciences, Northern Arizona University, Flagstaff, AZ 86011-5640 USA*, [2]*Division of Biological Sciences, The University of Montana, Missoula, MT 59812 USA*, [3]*Department of Respiratory Care, Boise State University, Boise, ID 83725 USA*, [4]*Department of Biology, Bates College, Lewiston, ME 04240 USA* and [5]*Division of Physiology, Department of Medicine, University of California San Diego, La Jolla, CA 92093-0623 USA*

*Author for correspondence (e-mail: steven.hempleman@nau.edu)

Accepted 14 June 2005

Summary

Biological rates in small animals are usually higher than those in large animals, yet the maximal rate of action potential (spike) generation in sensory neurons encoding rate functions is similar in all animals, due to the conserved genetics of voltage-gated ion channels. Therefore, sensory signals that vary at rates approaching maximal spike generation rate, as might occur in animals of diminished body size, may require specialized spike coding to convey this information. To test whether spike coding scales allometrically in sensory neurons monitoring signals that change frequency with body size, we recorded action potentials from 70 avian intrapulmonary chemoreceptors (IPC), respiratory neurons that detect lung CO_2 changes during breathing, in five different avian species ranging in size from body mass M_b = 0.045 kg (lovebirds) to 5.23 kg (geese). Since breathing frequency scales approximately to $M_b^{-1/4}$ (higher in small birds, lower in large birds), we reasoned that IPC discharge frequencies may also scale to maintain spike information transmission within each breath. We found that phasic action potential discharge pattern, as quantified by the peak discharge rate and the magnitude of spike frequency adaptation, scaled between $M_b^{-0.22}$ and $M_b^{-0.26}$, like breathing rate (P<0.05). Previously published values of peak discharge rate in IPC also fit this allometric relationship. We suggest that mass-dependent scaling of neural coding may be necessary for preserving information transmission with decreasing body size.

Key words: allometry, body size, bird, intrapulmonary chemoreceptors, neural coding.

Introduction

Biological rates, such as the frequencies of breathing, cardiac contraction, gait, and mass-specific metabolic rate, usually scale inversely to animal body mass M_b. Accordingly, small animals like hummingbirds and shrews have intrinsically higher biological rates than ostriches and elephants (Calder, 1996; Lindstedt and Calder, 1981; Schmidt-Nielsen, 1984). This is often explained as biological time (as opposed to clock time) running faster for small animals and slower for large animals. When quantified using the allometric scaling model, (y=aM_b^b), biological rates show quite consistent scaling in the range of $M_b^{-0.25}$ to $M_b^{-0.33}$; that is, they scale to the negative 1/4 to 1/3 power of body mass (Brown and West, 2000; Calder, 1996; Frappell et al., 2001; Lindstedt and Calder, 1981; Schmidt-Nielsen, 1984). In the allometric model, y is a biological trait, M_b is body mass, a is a constant associated with phylogenetic characteristics, and b is the mass exponent.

An exception to frequency scaling occurs in the nervous systems of animals. Maximal action potential (spike) generation rate in neurons is relatively fixed in animals of varying size because of the highly conserved genetics and kinetics of voltage-gated ion channels. Ion channel kinetics and gating are key determinants of transmembrane ionic fluxes, and control the width, shape and refractory periods of action potentials. The interplay of expressed ion channels in axonal membranes sets a practical upper limit for spike frequency at approximately 300 s^{-1} in most neurons, but normal discharge rates are usually much slower even in very small animals (Hille, 1992).

Action potential spike trains are the mechanism for long distance information transmission in the nervous system. In general, neural information may be 'rate coded,' with average spike rate over a time period encoding stimulus intensity, or 'time coded,' with the occurrence of a single spike (or spike burst) encoding the occurrence of a rapid stimulus transition (Rieke et al., 1999). Rate and time codes are not mutually exclusive: 'partially adapting' sensory neurons are common, and have both tonic (rate coded) and phasic (time coded) discharge responses (see below).

Rate codes are probably the most intuitive spike coding format in the nervous system (Rieke et al., 1999). This is the code observed in 'tonic' sensory receptors that detect slowly changing sensory input. However, a rate code requires transmission of relatively many action potentials to describe the sensory stimulus, because the stimulus amplitude is encoded as time-averaged spike discharge rate. Since it takes time to generate these action potentials, the maximal stimulus frequency that can be rate encoded is considerably less than the maximum possible spike discharge frequency.

As the stimulus frequency increases, a rate code becomes inadequate (not enough time for the needed number of spikes), but a timing code can still transmit information. In a timing code, the occurrence of one spike or a rapid burst of spikes indicates that an abrupt phasic change in stimulus intensity has occurred (Rieke et al., 1999). However, time coding is ineffective for indicating steady (tonic) stimulus levels.

The range of stimulus frequencies that can be encoded by a sensory neuron may be thought of as its 'bandwidth'. Since rate codes accurately represent low (tonic) stimulus frequencies, and timing codes accurately represent high (phasic) stimulus frequencies, the bandwidth of a neuron can be broadened by incorporating features of both rate and time coding. This broadening of bandwidth is seen in sensory receptors that are partially adapting – having both phasic and tonic responses.

Limited sensory bandwidth may have adverse fitness consequences if detection of fast sensory input is needed to avoid predation, detect prey or mates, or maintain homeostasis. It is not surprising, then, that several mechanisms for neural coding of rapid signals have evolved. These include the phasically responding (partially and rapidly adapting) receptors mentioned previously. Other mechanisms include specialized sensory organs that are 'tuned' to detect higher stimulus frequencies. For example, in the vertebrate ear, sensory hair cells arrayed along the basilar membrane of the cochlea use an anatomical place code (their position along the frequency-tuned membrane) to encode stimulus frequency, and a rate code (their spike discharge rate) to encode stimulus amplitude.

We hypothesized that some phasic physiological traits, like breathing rates, which scale to approximately $M_b^{-1/4}$ (Lindstedt and Calder, 1981), are slow enough in large animals to be adequately represented using a neural rate code, but are rapid enough in small animals to require at least some elements of a neural timing code for effective signal processing. If true, this would provide the first evidence for allometric scaling of neural coding. Clearly, spike rate codes are well known in sensory systems dealing with low frequency signals (tonic receptors), and spike timing codes are well known in sensory systems dealing with high frequency signals (phasic or adapting receptors); however, the transition between these two coding systems in a single sensory system due to variation in body mass (i.e. allometry of neural coding) has never been investigated. We tested for neural coding allometry by measuring action potential spike trains from sensory neurons (intrapulmonary chemoreceptors, IPC) that detect lung CO_2 oscillations linked to breathing rate, in birds ranging in body mass from 0.045 kg to 5.23 kg. We found that phasic action potential discharge pattern (peak discharge rate and magnitude of spike frequency adaptation, both in units of spikes s^{-1}) scaled between $M_b^{-0.23}$ and $M_b^{-0.26}$, like breathing rate. We suggest that body-mass-dependent changes in the neural coding of phasic signals preserves information transmission rates for high frequency signals in IPC (and perhaps other) sensory neurons.

Materials and methods

Experimental animals

The mean body mass (M_b) and number (N) of birds studied were as follows: lovebirds *Agapornis roseicollis* Vieillot, (M_b=0.045 kg, N=5), quail *Coturnix japonica* Temminck and Schlegel (M_b=0.192 kg, N=6), pigeons *Columba livia* Gmelin (M_b=0.446 kg, N=3), Pekin ducks *Anas platyrhynchos* L. (M_b=2.818 kg, N=9) and geese *Anser anser* L. (M_b=5.231 kg, N=5). All birds were obtained from commercial suppliers and maintained under normal vivarium conditions. Food was withheld from the larger birds overnight before they were used in experiments. Husbandry and experimental protocols were reviewed and approved by either the Institutional Animal Care and Use Committee at the University of California San Diego or that at Northern Arizona University.

Surgical preparation and unidirectional ventilation

Birds were restrained in dorsal recumbency and polyethylene catheters inserted into the left brachial artery and vein using a local anesthetic (Lidocaine HCl). Each bird was then anesthetized with sodium pentobarbital (20–90 mg kg^{-1} i.v. initially; supplementary doses of 4–15 mg kg^{-1} h^{-1} i.v. or as needed). In some quail, induction of surgical anesthesia with pentobarbital was followed by injections of urethane (1–2 mg min^{-1} i.v. or as needed). Arterial blood pressure and body temperature in most birds were continuously monitored during and following induction of deep surgical anesthesia (Kilgore et al., 1985). Colonic temperature (T_b) was regulated to 41±1°C in all birds except lovebirds, where T_b was regulated to 40±1°C.

Unidirectional ventilation followed previously described procedures (Hempleman and Bebout, 1994; Hempleman et al., 2000). In birds where each lung was independently ventilated, airflow through the two lungs exceeded reported ventilatory flow rates by an average factor of 1.1–1.9. All lovebirds, most of the quail and two ducks were unidirectionally ventilated with a continuous stream of warmed, humidified gas that was delivered *via* an endotracheal tube, and exited the opened interclavicular air sac (Hempleman et al., 2000; Shoemaker and Hempleman, 2001). Insufflation rates exceeded published ventilatory flow rates in these birds by a factor of 4–5. Carbon dioxide was added to the ventilatory gas stream going to the left lung or through the trachea with an electronic valve to make step changes in lung CO_2 concentration between low

(0–1%) and high (5%–7%; Hempleman and Bebout, 1994; Hempleman et al., 2000). Arterial blood gases were periodically assessed to ensure the adequacy of ventilation. Arterial samples were anaerobically drawn into heparinized syringes and analyzed with a blood gas system (Hempleman and Bebout, 1994). CO_2 and O_2 concentrations in the ventilation streams were measured with a respiratory mass spectrometer or separate gas analyzers (Hempleman and Bebout, 1994).

Neural recording

Extracellular single-unit action potentials were recorded from fine vagal filaments under mineral oil using Pt-Ir and Ag-AgCl electrodes coupled with a Grass HIP511 high impedance differential probe to a Grass P511K AC preamplifier (West Warwick, RI, USA). Vagal filaments were divided by micro-dissection until action potentials from only a single IPC were evident in the electrical recording. IPC were identified by their prompt response to step reductions in ventilatory CO_2, and single IPC action potentials were identified by the constant shape and amplitude of their spike waveform (Hempleman and Bebout, 1994; Hempleman et al., 2000; Shoemaker and Hempleman, 2001). Occurrence times of action potentials and CO_2 stimulus steps were recorded on-line using an Intel 8085-based interrupt driven assembly language program sampling at 14 500 s^{-1} (Hempleman and Bebout, 1994; Hempleman et al., 2000; Shoemaker and Hempleman, 2001). Data were analyzed off-line to produce cycle triggered stimulus histograms (averaged spike frequency *vs* time) and raster plots (spike occurrence *vs* time) of IPC spike activity (e.g. Fig. 1). Statistical analyses (ANOVA and linear regression) were performed using SAS JMP-IN (v.4) on a Microsoft Windows 2000 platform.

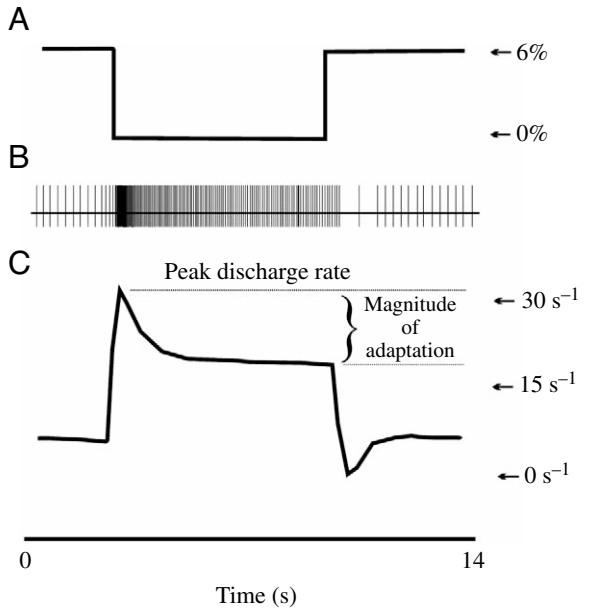

Fig. 1. The analysis method for determining phasic peak discharge rate and magnitude of spike frequency adaptation of individual intrapulmonary chemoreceptors. (A) The CO_2 stimulus waveform delivered to the lungs in the ventilatory gas. (B) Raster plot of spike occurrence times as vertical hash marks (this example was recorded from a lovebird IPC). (C) A schematic representation of spike discharge frequency *vs* time – a cycle triggered stimulus histogram. Definitions of peak frequency and magnitude of spike frequency adaptation are indicated (both measurements are in units of frequency: s^{-1}).

Allometric equations for phasic discharge during down-steps in ventilatory CO2

Cycle triggered stimulus histograms from each IPC were used to tabulate species mean values of two indices of phasic discharge to a CO_2 down-step: (1) peak discharge rate and (2) magnitude of spike frequency adaptation, both in units of inverse time (s^{-1}; Fig. 1C). Spike frequency adaptation is the burst-like roll-off in spike frequency after a stimulus step despite maintained stimulus intensity (Hille, 1992). These indices were compared among species with ANOVA. We fit measurements of body mass (M_b) and peak discharge rate or magnitude of spike frequency adaptation (y) to the allometric equation ($y=aM_b^b$) using a log-log regression [$\log(y)=b\times(\log M_b)+\log(a)$] to obtain the power function (b) and the proportionality constant (a).

Phylogenetically independent contrast analysis of phasic discharge data

Since linear regression of multi-species data assumes phylogenetic independence of subjects, violations of independence may affect the accuracy and confidence limits of the calculated mass exponent (b) and phylogenetic constant (a) (Garland et al., 1993). Some birds in our study had closer phylogenetic ties than others (Frappell et al., 2001), so we tested the effect of phylogenetic relatedness using PDAP (Phenotypic Diversity Analysis Programs), version 6.0 (Garland et al., 1993, 1999; Garland and Ives, 2000) running in DOS on a Pentium III based Dell Optiplex GX150 PC. Phylogenetically corrected allometric mass exponents and constants (with their standard errors) calculated with PDAP are reported below.

Results

We logged 51 437 action potentials in spike trains from 70 IPC in five different species (goose, duck, pigeon, quail, and lovebird). Table 1 summarizes numbers of IPC, mean body mass, mean peak discharge frequency, mean spike frequency adaptation, and associated standard errors for the IPC from these five species. To our data, we added published peak IPC discharge frequencies for a variety of species from the literature (Table 2). All available data on peak IPC discharge frequency summarized in Table 2 were included in allometric calculations and plots of peak discharge frequency (as indicated).

In smaller birds, abrupt step decreases in lung CO_2 produced higher peak IPC discharge rates and increased magnitude of spike frequency adaptation ($P<0.05$; Fig. 2, Table 3). The peak

Table 1. *Mean body mass, mean peak IPC discharge frequency and mean IPC frequency adaptation of species in the present study*

Species	Body mass (kg)	Number of IPC	Peak discharge frequency (s^{-1})	Frequency adaptation (s^{-1})
Goose	5.231	13	15.7±1.9	7.9±1.4
Pekin duck	2.818	17	13.8±2.6	7.1±1.8
Pigeon	0.446	3	33.6±11.0	17.9±5.9
Quail	0.192	20	36.0±3.1	16.4±2.9
Lovebird	0.045	17	47.0±6.8	24.2±4.0

Peak discharge and adaptation values are means ± S.E.M.
IPC, intrapulmonary chemoreceptors.

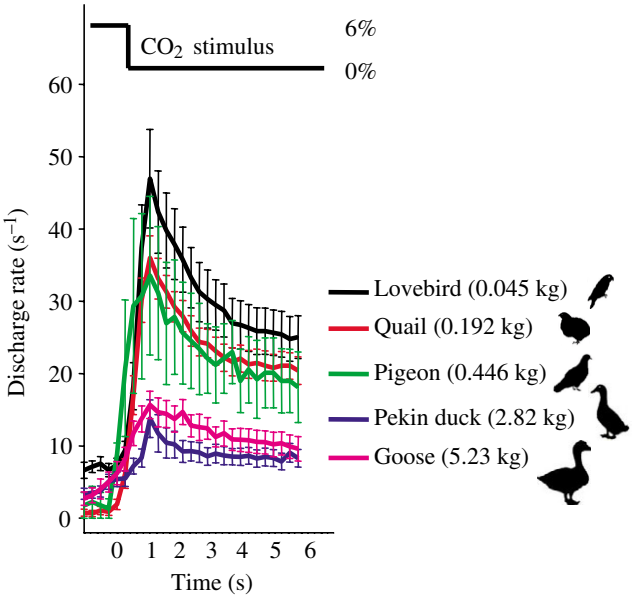

Fig. 2. IPC discharge rate (s^{-1}; means ± S.E.M.) *vs* time for each species. Smaller birds had larger phasic chemoreceptor responses to the CO_2 stimulus down-step. Mean peak discharge frequencies and the mean magnitude of spike frequency adaptation were calculated from these data as described in Fig. 1, and shown in Figs 3 and 4.

spike discharge rates were inversely related to body mass according to the power-law relationship ($y=aM_b^b$). With CO_2 step decreases, log-log regression analysis without phylogenetic correction showed that peak IPC discharge rate scaled to $M_b^{-0.235}$ (Fig. 3, heavy black line, $r^2=0.846$), and the magnitude of IPC spike frequency adaptation scaled to $M_b^{-0.263}$ (Fig. 4, heavy black line, $r^2=0.904$). Each of the calculated mass exponents (b) were different from zero ($P<0.001$), but were not different from –0.25 ($P>0.4$). Mean parameter values (± S.E.M.) for the mass exponents (b) and proportionality constants (a) are shown in Table 3.

Fig. 3 shows the mean peak IPC discharge rates from the five species we studied (symbols wholly or partly red) and also includes mean peak IPC discharge rates from the avian species published in the literature (emu, chicken, muscovy duck, mallard duck and Pekin duck: symbols wholly or partly in

Table 2. *Mean body mass and mean peak IPC discharge frequency for species included in allometric analyses of peak discharge frequency (Fig. 3, Table 3)*

Species	Body mass (kg)[a]	Peak discharge frequency (s^{-1})[b]	Literature source
Emu	26.5 (1)	10.2 (12)	Burger et al., 1976
Goose	5.231 (5)	15.7 (13)	Present study
Pekin/Mallard duck			
Pekin	2.818 (9)	13.8 (17)	Present study
Pekin	3.1 (10)	36 (42)	Tallman and Grodins, 1982
Pekin	2.3 (8)	31 (25)	Berger et al., 1980
Mallard	1.25 (15)	35 (16)	Shoemaker and Hempleman, 2001
Mallard	1.25 (16)	34.7 (15)	Hempleman et al., 2000
Weighted average	1.99[c]	30.3[d]	
Chicken	1.7 (12)	26 (16)	Gleeson, 1985
	1.4 (12)	37.3 (20)	Nye et al., 1982
Weighted average	1.55[c]	32.3[d]	
Muscovy duck	1.5 (6)	23 (57)	Fedde and Scheid, 1976
Pigeon	0.446 (3)	33.6 (3)	Present study
Quail	0.192 (6)	36.0 (20)	Present study
Lovebird	0.045 (5)	47.0 (17)	Present study

IPC, intrapulmonary chemoreceptors.
Numbers of [a]birds, [b]IPC are given in parentheses.
[c]Weighted by number of birds.
[d]Weighted by number of IPC.

Table 3. *Allometric exponents, coefficients, equations and* r^2 *values for peak discharge frequency and spike frequency adaptation uncorrected and corrected for phylogenetic relatedness*

Parameter	Number of species	Slope	Log intercept	Allometric equation	r^2
y=peak discharge frequency (s^{-1})					
Uncorrected	8	–0.235±0.041[a]	1.424±0.033[a]	$y=26.6M_b^{-0.235}$	0.846
Phylogenetically corrected	8	–0.231±0.060[a]	1.411±0.070[a]	$y=25.8M_b^{-0.231}$	0.715
y=spike frequency adaptation (s^{-1})					
Uncorrected	5	–0.263±0.049[a]	1.054±0.039[a]	$y=11.3M_b^{-0.263}$	0.904
Phylogenetically corrected	5	–0.224±0.072[b]	1.076±0.068[a]	$y=11.9M_b^{-0.224}$	0.761

Slope and intercept values are means ± S.E.M.
In the allometric equations, M_b=body mass in kg.
[a]$P<0.05$; [b]$P=0.055$.

green). One species, *Anas platyrhynchos*, representing the wild mallard duck and domestic Pekin duck, was studied by us and also by others (Table 2). The average of all mean peak discharge rates for *Anas platyrhynchos* IPC, weighted by the number of observations in each study, is shown as a green square with a red border in Fig. 3. Regression analyses included all data plotted in Fig. 3.

Phylogenetic correction produced negligible changes in the allometric regression equations for peak frequency and the magnitude of spike frequency adaptation, but did increase the estimates of the standard error (Table 3). With CO_2 step decreases, log-log regression analysis with phylogenetic correction showed that peak IPC discharge rate scaled to $M_b^{-0.231}$ (Fig. 3, heavy gray line, $r^2=0.715$), and the magnitude of IPC spike frequency adaptation scaled to $M_b^{-0.224}$ (Fig. 4, heavy gray line, $r^2=0.761$). The phylogenetically corrected mass exponent for peak frequency was again different from zero ($P<0.05$), but the 95% confidence interval for the corrected magnitude of spike frequency adaptation mass exponent marginally included zero ($P=0.055$). This is considered further in the Discussion.

We observed both tonic IPC and phasically adapting IPC in all of the species studied; however, the magnitude of the adaptation differed among species ($P<0.05$), as noted above and shown in Figs 2 and 4. Fig. 5A shows spike discharge characteristics of a partially adapting quail IPC: it has a prompt on-response to the stimulus, and the magnitude of spike frequency adaptation is large. Fig. 5B shows a minimally adapting (tonic) quail IPC from our study: it

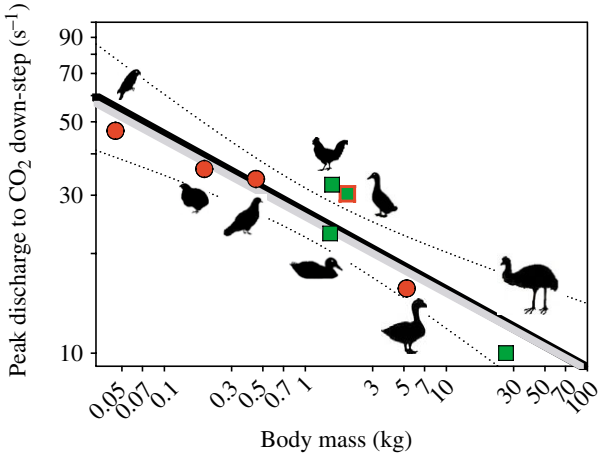

Fig. 3. Allometric plot of peak chemoreceptor discharge rate *vs* body mass (Table 2). The heavy black regression line was calculated without phylogenetic correction (dotted line indicates 95% confidence interval); the heavy gray regression line was calculated with phylogenetic correction (see text). Regression parameters are summarized in Table 3. Mean values measured in this study are shown in red (lovebird, quail, pigeon, and goose). Mean values from the literature are shown in green (chicken, muscovy duck, emu; see text). The red + green square is the mean value for *Anas platyrhynchos* (represented by mallard and Pekin ducks) combined from the literature and this study (Table 2). Silhouettes identify specific data points and are not scaled to actual bird size.

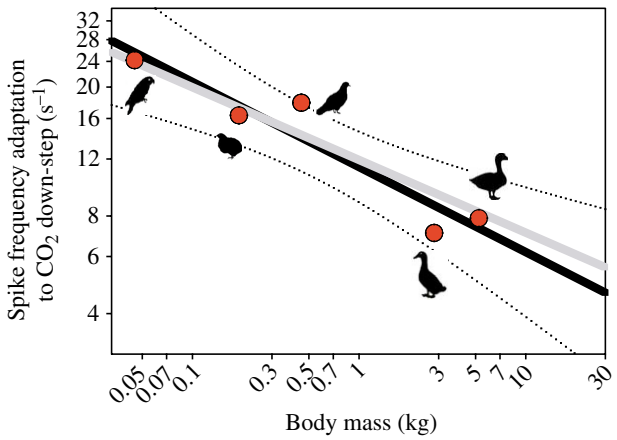

Fig. 4. Allometric plot of chemoreceptor spike frequency adaptation *vs* body mass (Table 1). The heavy black regression line was calculated without phylogenetic correction (dotted line indicates 95% confidence interval); the heavy gray regression line was calculated with phylogenetic correction (see text). Regression parameters are summarized in Table 3. Values shown are all from this study: lovebird, quail, pigeon, Pekin duck and goose (see text). Silhouettes identify specific data points and are not scaled to actual bird size.

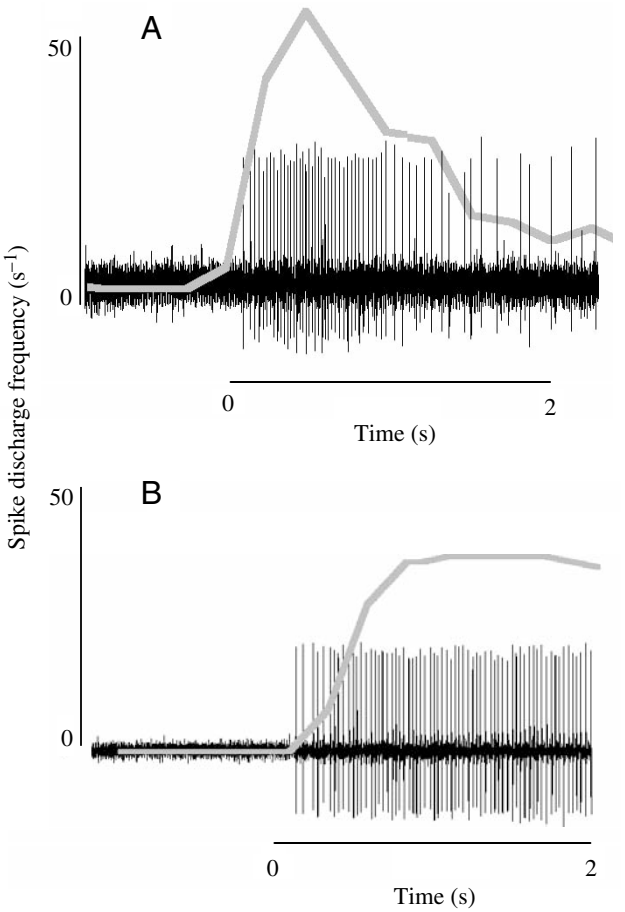

Fig. 5. Examples of partially adapting (A) and tonic (B) quail IPC responding to an abrupt inspired CO_2 down-step. Measured spike trains are shown in black. The heavy gray line shows chemoreceptor discharge rate from cycle triggered stimulus histogram averaged over 0.25 s intervals. We found examples of tonic and partially adapting chemoreceptors in all species studied, but IPC with large magnitude adaptation and higher peak discharge rates were more common in small birds, and IPC with lower peak discharge rates and smaller magnitude adaptation were more common in large birds (see text).

maintains a steady discharge at a given CO_2 stimulus, with little adaptation.

Discussion

The nervous system transduces and analyzes a rich array of sensory inputs that are necessary for homeostasis. Even within a single sensory modality, important temporal (rate-of-change) and amplitude (intensity) features of sensory stimuli may range over many orders of magnitude. Psychophysical observations like the Weber–Fechner Law describe logarithmic scaling of intensity perception with a change in stimulus strength. This logarithmic amplitude scaling helps explain the observed sensitivity to a broad amplitude bandwidth of stimulus intensities. In a similar way, we report here that scaling of spike coding in single sensory neurons (avian IPC) provides a mechanism for augmenting temporal bandwidth (the range of stimulus frequencies that can be encoded by receptor discharge) to match important temporal attributes of the stimulus. Our observation takes the form of an allometric (log-log) scaling of peak discharge rate and the magnitude of spike frequency adaptation to body mass.

For effective sensory feedback, spike trains of IPC must encode information about lung CO_2 that oscillates between ~0% and ~6% at the normal breathing frequency, which varies with metabolic rate and size (Powell et al., 1981). We found that the allometric scaling of IPC peak frequency and the magnitude of IPC spike frequency adaptation ranged from $M_b^{-0.224}$ to $M_b^{-0.263}$, which matched the allometric scaling of breathing rate at about $M_b^{-1/4}$. On the one hand this might be expected because mass-scaling exponents of this size and sign are characteristic of most biological frequencies (e.g. heart rate, breathing rate, gait frequency). However, to our knowledge this is the first time that allometric scaling of phasic peak spike discharge frequency and the magnitude of spike frequency adaptation has been reported in any class of neurons. The observation suggests a mechanism for continuous adjustment of neural coding in sensory spike trains, from a rate code when stimulus signals are of low frequency relative to the maximal possible action potential discharge rate, towards a time code when stimulus signals driving action potential discharge have a higher frequency. Over the body mass range we studied here, most allometric adjustments to IPC discharge occurred in terms of peak frequency. However, the significantly increased magnitude of spike frequency adaptation in smaller birds also suggests the emergence of rate coding in their IPC spike trains.

Scaling of peak discharge frequency to phasic stimulation

We propose that scaling of peak IPC discharge rate (spikes s^{-1}) with $M_b^{-1/4}$ is an important feature of IPC neural function. IPCs detect breath-by-breath fluctuations in lung CO_2, and transmit spike-encoded feedback information to the brainstem to help match breathing pattern to metabolic demands (Hempleman and Posner, 2004). Because the frequency of CO_2 fluctuations sensed by IPC is set by the breathing rate (breaths s^{-1}), which scales to $M_b^{-1/4}$, and this is matched by IPC peak discharge frequency (spikes s^{-1}), which also scales to $M_b^{-1/4}$, our results indicate that the mean number of IPC spikes transmitted per breath [(spikes s^{-1})/(breaths s^{-1})=(spikes breath^{-1})] is approximately independent of body mass [$(M_b^{-1/4})/(M_b^{-1/4})=M_b^0$]. Because action potentials are the fundamental unit of information transfer along axons, the higher peak discharge rates in IPC of smaller birds help compensate for the smaller birds' intrinsically shorter breath durations and higher breathing rates.

Matching spike code to biological time

An example of the temporal challenge of increased breathing rate on IPC spike transmission is shown in Fig. 6, modified from Stoll et al. (1971). Here, spike discharge from a chicken IPC was recorded while the bird was ventilated with a variable

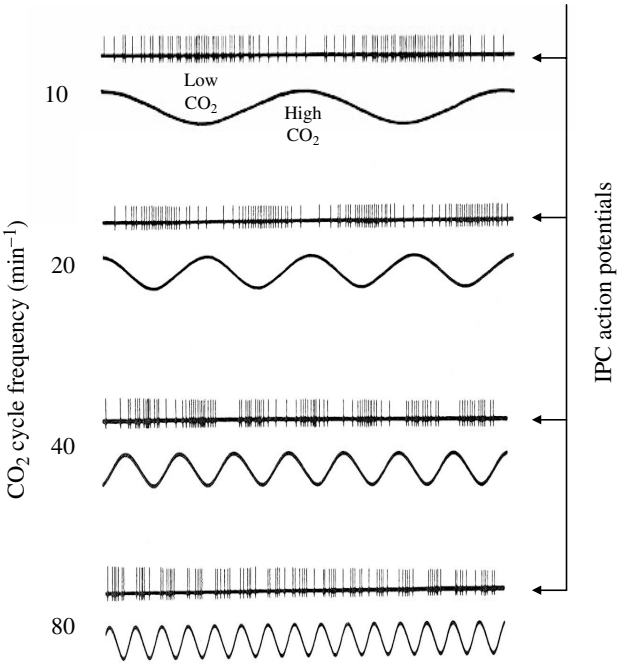

Fig. 6. The effect of CO_2 oscillation frequency on IPC action potential discharge in a 1.9 kg domestic chicken (modified from Stoll et al., 1971). This IPC tracked 20 min^{-1} CO_2 oscillations that are close to its normal breathing rate more faithfully than faster oscillations (see text).

flow of CO_2 (0.4–1.6%) at 10, 20, 40 and 80 cycles min^{-1}. The average breathing rate for a 1.9 kg chicken is about 20 breaths min^{-1} (Frappell et al., 2001). As shown in Fig. 6, decreasing lung CO_2 causes increases in IPC discharge rate (Hempleman and Posner, 2004; Molony, 1974). At 20 cycles min^{-1}, changes in IPC spike frequency faithfully follow the sinusoidal variations of carbon dioxide, and there are ample numbers of spikes generated during the cyclic increases and decreases in CO_2 to encode the associated changes in CO_2 as changes in spike frequency (i.e. spike rate coding; Rieke et al., 1999). However, at higher cycle rates the changes in spike frequency become less distinct, and there is less time for spike transmission within each cycle. At 80 cycles min^{-1}, spike rate coding is sparse. If this particular IPC were capable of a higher peak spike frequency (as naturally occurs in IPC of smaller birds; Tables 1, 2), it might have retained its ability to rate-encode CO_2 changes at cycle rates of 80 min^{-1} or above. The resting breathing rate for a 0.004 kg hummingbird is much higher than the frequencies shown here, about 173 breaths min^{-1} (Frappell et al., 2001), so IPC in small birds somehow meet this temporal challenge.

Another way to view the temporal challenge imposed by $M_b^{-1/4}$ scaling of breathing rate and $M_b^{1/4}$ scaling of breath duration on IPC sensory transmission is illustrated in Fig. 7. IPC spike trains (one example from each species we studied, shown as raster scans from original data) are arrayed perpendicular to the ordinate and spaced vertically according to the logarithm of the species' body mass. Actual spike occurrence times are spaced along the abscissa of each raster. An abrupt decrease in lung CO_2 occurred at 0 s for each IPC (heavy black line), which stimulated spike discharge. The broad gray 'V' superimposed on the graph shows the impact of $M_b^{1/4}$ scaling of breath duration. The 5.23 kg goose's breath duration was set arbitrarily at 2 s (corresponding to a breathing rate of 30 min^{-1}, which is higher than resting but less than maximum). Accordingly, $M_b^{1/4}$ scaling of the 0.446 kg pigeon's breath duration yielded 1.08 s, and the 0.045 kg lovebird scaled to 0.608 s. Note that the narrowing 'V' (diminishing breath duration) with decreasing body mass leaves less time per breath for sensory spike transmission in

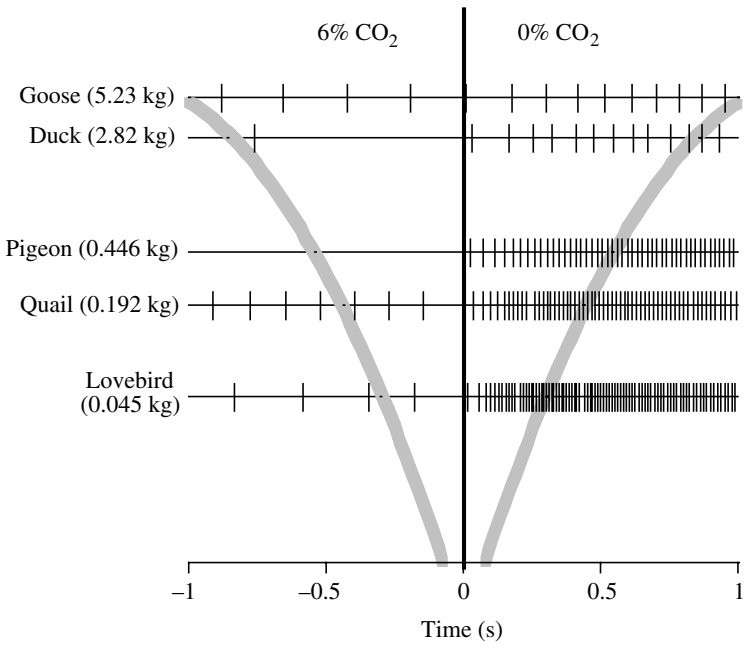

Fig. 7. Breathing frequency in birds scales approximately to $M_b^{-1/4}$, and breath duration scales approximately to $M_b^{1/4}$ (Frappell et al., 2001; Lindstedt and Calder, 1981). $M_b^{1/4}$ scaling of breath duration is indicated schematically by the heavy gray 'V' lines on the diagram: larger birds have relatively longer breaths, and smaller birds have relatively shorter breaths. Representative spike recordings of IPC from five species responding to a CO_2 downstep at t=0 (heavy black line) are overlayed on the figure, and are spaced vertically according to body mass of birds in which they were measured. The composite figure shows the general scaling relationship between spike discharge and breath duration. Note that as relative breath duration decreases with decreased body mass, peak chemoreceptor discharge rate and the magnitude of spike frequency adaptation increase. Note also that some IPC were silenced by 6% CO_2; this was idiosyncratic of individual IPC and not species or mass related. On average, larger birds had lower peak chemoreceptor discharge rates, but their longer breaths give IPC ample time to transmit spike information about lung CO_2 changes.

smaller species, but that the increased spike discharge rate seen in IPC of smaller birds (approximately proportional to $M_b^{-1/4}$) largely compensates for this.

Scaling the magnitude of spike frequency adaptation

We also observed $M_b^{-1/4}$ scaling of the magnitude of spike frequency adaptation in IPC, which suggests yet another mechanism for transmitting information about high frequency CO_2 signals: the magnitude of IPC spike frequency adaptation is larger in smaller birds (Table 1, Figs 2, 4). Adapting sensory neurons (e.g. Fig. 5A) produce spikes in response to phasic changes in their adequate stimulus (which in IPC is the abrupt down-step of intrapulmonary CO_2 that sweeps through the lung during each inspiration), but are less responsive to tonic stimuli. Spike frequency adaptation helps focus on the phasic features of a stimulus and encodes them as relatively short bursts of action potentials signaling the stimulus transition. This bursting is thought to represent a 'timing code', which allows a few spikes from a single sensory fiber to convey information about higher stimulus frequencies than would be possible with the rate code described above (Rieke, 1999).

We noticed that all birds generally had both partially adapting IPC and tonic IPC (e.g. Fig. 5A,B), but in varying proportions depending on the birds' body size. As seen in Fig. 2, the averaged CO_2 step responses of IPC in large birds were mostly tonic in character with a small magnitude of spike frequency adaptation (perhaps emphasizing IPC spike rate coding at their slower breathing rates). In contrast, the averaged CO_2 response of IPC in smaller birds had larger magnitudes of spike frequency adaptation and less tonic character (perhaps emphasizing IPC spike time coding at their higher breathing rates). If this allometric relationship extends to the smallest *Aves*, we predict that 4 g hummingbirds should have IPC with exceptionally large magnitudes of spike frequency adaptation and peak discharge to phasic stimuli, and little tonic character.

Spike frequency adaptation can be characterized by its magnitude (discussed above) and also by its rate. The rate of adaptation quantifies how rapidly spike discharge declines after a step change to a higher stimulus level. Even though the magnitude of spike frequency adaptation was mass dependent among the species ($P<0.05$), the relative rate of spike frequency adaptation (% change in discharge frequency over time) was not ($P>0.05$). This is apparent in Fig. 2.

Phylogenetic independent contrasts

We were concerned that phylogenetic non-independence among our subject animals may have biased our estimates of allometric body mass exponents. However, correcting the estimates using the Phenotypic Diversity Analysis Programs ('PDAP'; Garland et al., 1993, 1999; Garland and Ives, 2000) resulted in essentially identical mass exponents for scaling both peak frequency and spike frequency adaptation, with somewhat larger standard errors and confidence limits (Table 3). With phylogenetic correction, the mass exponent for peak discharge remained significantly different from zero ($P<0.05$) but the exponent for spike frequency adaptation became marginally insignificant ($P=0.055$). While post-correction insignificance of the adaptation exponent may indicate true mass independence, it is perhaps more likely related to sample size. The adaptation exponent value remained essentially the same at –0.22 after phylogenetic correction; and because it is common for variance of estimated exponents to increase after phylogenetic correction (Frappell et al., 2001), the marginal insignificance (5 parts in 1000) may represent a type II error, which could be remedied by increasing sample size. In the future we hope to increase statistical power with new experiments on larger or smaller birds to further test the phylogenetically corrected adaptation exponent.

Possible biological basis for spike frequency scaling

Since receptor endings of IPC are probably the sites of spike initiation, but IPC receptor endings have never been isolated or studied, we can only speculate on the origins of allometric differences in spike coding. General membrane biophysics suggests that peak discharge rate and spike frequency adaptation should be dependent on the magnitude of the generator potential produced at the sensory endings, and on the ability of the sensory neuron to generate and recover from action potentials extremely rapidly. These actions would be influenced by the type, number and distribution of ion channels, transmembrane ion exchangers, and active membrane pumps expressed in the receptor endings, which may in turn be affected by the developmental programmes for animals of different sizes. To test these hypotheses, IPC receptor endings must be identified, and transmembrane voltage and current recordings made from functioning IPC. This remains a problem for future study.

Conclusions

Maximal action potential frequency is limited in most neurons to about 300 s^{-1} or less, due to the relatively invariant genetics of voltage-gated Na^+ and K^+ channels underlying spike generation (Hille, 1992). Spike-frequency bandwidth limitation is known to cause variations in spike coding strategy when comparing sensory receptors that normally respond to tonic signals, to sensory receptors that normally respond to phasic signals. Well-known examples, especially in mechanoreceptors, include the 'rate code' commonly associated with slowly adapting receptors, and the 'timing code' commonly associated with rapidly adapting receptors (Rieke et al., 1999). Here we provide evidence for a systematic allometric shift in the neural spike code of avian intrapulmonary chemoreceptors observed in birds of body size varying over 2.7 orders of magnitude. The magnitudes of peak spike frequency and spike frequency adaptation both scaled with body mass to approximately $M_b^{-1/4}$. This scaling matches the known $M_b^{-1/4}$ scaling of breathing rate with body mass, and may help preserve the amount of spike-coded information available as breath duration decreases with body mass.

We thank Stan Lindstedt, Dona Boggs, Kiisa Nishikawa, Jenna Monroy, Jason Pilarski and two anonymous reviewers for comments and discussion about the manuscript, and Leslie Hempleman for technical assistance. We thank Dr Ted Garland for providing the PDAP programs. Support from the National Institutes of Health to S.C.H and F.L.P., and from the National Science Foundation to D.L.K. and S.C.H., is gratefully acknowledged. Lastly, we would like to acknowledge the contributions of Ray E. Burger and M. Roger Fedde, whose pioneering studies of intrapulmonary chemoreceptors in birds provided the foundation for this study.

References

Berger, P. J., Tallman, R. D. and Kunz, A. L. (1980). Discharge of intrapulmonary chemoreceptors and its modulation by rapid FI_{CO_2} changes in decerebrate ducks *Respir. Physiol.* **42**, 123-130.

Brown, J. H. and West, G. B. (2000). *Scaling in Biology*. New York: Oxford University Press.

Burger, R. E., Coleridge, J. C. G., Coleridge, H. M., Nye, P. C. G., Powell, F. L., Ehlers, C. and Banzett, R. B. (1976). Chemoreceptors in the paleopulmonic lung of the emu: discharge patterns during cyclic ventilation. *Respir. Physiol.* **28**, 249-259.

Calder, W. A. (1996). *Size, Function, and Life History*. Mineola, NY: Dover.

Fedde, M. R. and Scheid, P. (1976). Intrapulmonary CO_2 receptors in the duck: IV Discharge pattern of the population during a respiratory cycle. *Respir. Physiol.* **26**, 223-227.

Frappell, P. B., Hinds, D. S. and Boggs, D. F. (2001). Scaling of respiratory variables and the breathing pattern in birds: an allometric and phylogenetic approach. *Physiol. Biochem. Zool*. **74**, 75-89.

Garland, T. and Ives, A. R. (2000). Using the past to predict the present: confidence intervals for regression equations in phylogenetic comparative methods. *Am. Nat.* **155**, 346-364.

Garland, T., Dickerman, A. W., Janis, C. M. and Jones, J. A. (1993). Phylogenetic analysis of covariance by computer simulation. *Syst. Biol.* **42**, 265-292.

Garland, T., Midford, P. E. and Ives, A. R. (1999). An introduction to phylogenetically based statistical methods, with a new method for confidence intervals on ancestral states. *Am. Zool.* **39**, 374-388.

Gleeson, M. (1985). Changes in intrapulmonary chemoreceptor discharge in response to the adjustment of respiratory pattern during hyperventilation in domestic fowl. *Q. J. Exp. Physiol.* **70**, 503-513.

Hempleman, S. C. and Bebout, D. E. (1994). Increased venous P_{CO_2} enhances dynamic responses of avian intrapulmonary chemoreceptors. *Am. J. Physiol.* **266**, R15-R19.

Hempleman, S. C. and Posner, R. G. (2004). CO_2 transduction mechanisms in avian intrapulmonary chemoreceptors: experiments and models. *Respir. Physiol. Neurobiol.* **144**, 203-214.

Hempleman, S. C., Rodriguez, T. A., Bhagat, Y. A. and Begay, R. S. (2000). Benzolamide, acetazolamide, and signal transduction in avian intrapulmonary chemoreceptors. *Am. J. Physiol.* **279**, R1988-R1995.

Hille, B. (1992). *Ionic Channels of Excitable Membranes*, 2nd edn. Sunderland, MA: Sinauer Associates.

Kilgore, D. L., Faraci, F. M. and Fedde, M. R. (1985). Ventilatory and intrapulmonary chemoreceptor sensitivity to CO_2 in the burrowing owl. *Respir. Physiol.* **62**, 325-339.

Lindstedt, S. L. and Calder, W. A. (1981). Body size, physiological time, and longevity of homeothermic animals. *Q. Rev. Biol*. **56**, 1-16.

Molony, V. (1974). Classification of vagal afferents firing in phase with breathing in *Gallus domesticus*. *Respir. Physiol.* **22**, 57-76.

Nye, P. C. G., Barker, M. R. and Burger, R. E. (1982). Chicken intrapulmonary chemoreceptor discharge frequency reduced by increasing rate of repetitive P_{CO_2} changes. *Q. J. Exp. Physiol.* **67**, 607-615.

Powell, F. L., Geiser, J., Gratz, R. K. and Scheid, P. (1981). Airflow in the avian respiratory tract: variations of O_2 and CO_2 concentrations in the bronchi of the duck. *Respir. Physiol*. **44**, 195-213.

Rieke, F., Warland, D., de Ruyter van Stevenick, R. and Bialek, W. (1999). *Spikes: Exploring the Neural Code*. Cambridge, MA: The MIT Press.

Schmidt-Nielsen, K. (1984). *Scaling: Why is Animal Size so Important?* New York: Cambridge University Press.

Shoemaker, J. M. and Hempleman, S. C. (2001). Avian intrapulmonary chemoreceptor discharge rate is increased by anion exchange blocker 'DIDS'. *Respir. Physiol.* **128**, 195-204.

Stoll, P. J., Estavillo, J. A., Osborne, J. L. and Burger, R. E. (1971). Control theory applied to the chemical regulation of breathing. *Chem. Eng. Prog.* **67**, 202-210.

Tallman, R. D. and Grodins, F. S. (1982). Intrapulmonary CO_2 receptor discharge at different levels of venous P_{CO_2}. *J. Appl. Physiol.* **53**, 1386-1391.